International Journal of Pharmaceutics 372 (2009) 147–153

Contents lists available at ScienceDirect

International Journal of Pharmaceutics

journal homepage: www.elsevier.com/locate/ijpharm

Pharmaceutical Nanotechnology

Forces between insulin microspheres and polymers surfaces for a dry powder inhaler

Steve C. Strathmann[a], Mary Ann Murphy[a], Bruce A. Goeckner[b], Phillip W. Carter[c], John-Bruce D. Green[c,*]

[a] Department of Particle Science in the Technology Resources Division, Baxter Healthcare Corporation, Round Lake, IL 60073, United States
[b] Department of Advanced Technology Resources in the Medication Delivery Division, Baxter Healthcare Corporation, Round Lake, IL 60073, United States
[c] Department of Exploratory Sciences in the Technology Resources Division, Baxter Healthcare Corporation, Round Lake, IL 60073, United States

ARTICLE INFO

Article history:
Received 29 September 2008
Received in revised form 30 December 2008
Accepted 6 January 2009
Available online 17 January 2009

Keywords:
Colloidal probe microscope
Atomic force microscope
Insulin microspheres
Dry powder inhaler

ABSTRACT

Here we demonstrate the use of a colloidal probe atomic force microscope (AFM) to compare the interactions between a model protein microsphere (insulin) and a set of common device polymers (polytetrafluoroethylene, polyethylene and polypropylene) with and without antistatic additive. For inhalation-based delivery devices the solid protein microspheres will interact with the device surfaces under ambient atmospheric conditions, and as such we studied the particle device interaction at a range of relative humidities. The results clearly discriminate between the five different polymer choices, and the impact of the antistatic additive. Although the mechanistic understanding is incomplete, it is evident that the polypropylene with antistatic additive gives consistent and relatively small interaction forces over the entire humidity range. The other polymer surfaces have humidity ranges where the pull-off forces are substantially greater. At 80% relative humidity, the insulin-polymer adhesion forces were similar for all the polymers probably due to the dominance of static charge mitigation and surface hydration effects. Overall, direct measurement of adhesion forces between pharmaceutical microspheres and container substrates can help direct rational choice of plastics/coatings for medical devices.

1. Introduction

Design and implementation of devices for medication delivery invariably involves the exposure of the active pharmaceutical to device surfaces and interfaces. The interactions between the pharmaceutical components and these interfaces can have a profound impact on the performance of the devices, with beneficial or deleterious results. For example, strong interactions can result in retention of the drug on the device surface, which leads to wasted material, irreproducible delivery, and inconsistent dosages. As a result, understanding and controlling these interfacial forces can assist with a more effective device design and function that translates to an improved quality of treatment for patients.

Recent improvements in recombinant methods have produced higher quality proteins and peptides as pharmaceutical agents. The physical chemistry of peptides and larger, more complex and sensitive proteins make conventional formulation and delivery through tablets and oral/GI tract inappropriate, and to date most have been administered via injection. Over the last couple of decades there has been significant effort aimed at pulmonary delivery to treat systemic diseases (Mandal, 2005). Due to the high surface area of the alveoli membrane, transport from the lung into the bloodstream is rapid, and the ease of use and comfort of administration is preferable to the pain of injections. Unfortunately, there are also several difficulties including physiological barriers to absorption and irreproducibility of administration. Nonetheless, the increased supply of high quality proteins and peptides as potential therapeutic agents has added to the interest in overcoming these obstacles and further developing inhalation-based delivery.

In this study, we have focused on material selection during device design for pulmonary delivery of proteins, specifically the use of a dry particle inhaler to deliver insulin. In a dry particle inhaler (Agu et al., 2001; Mandal, 2005; Hickey et al., 2007), the patient would load a pre-packaged measured dose of the drug into the device, and then the patient would inhale at a steady rate. The process of inhaling combined with the particle morphology and the architecture of the inhaler would disperse the drug and carry it into the alveolar space of the patient. The dynamics of dispersing the dry powder depends upon numerous variables including: powder morphology (size and shape), powder mechanical properties (e.g. elastic modulus), powder surface chemistry (free energy, hydrophobicity, etc.), humidity, device surface roughness, and device surface chemistry. In our study, the particles

* Corresponding author. Tel.: +1 847 270 6508; fax: +1 847 270 5449.
E-mail address: john_bruce_green@baxter.com (J.-B.D. Green).

0378-5173/$ – see front matter © 2009 Elsevier B.V. All rights reserved.
doi:10.1016/j.ijpharm.2009.01.004

are insulin microspheres with typical diameters in the 2–4 μm range, an optimum size for reaching the alveoli in the respiratory zone.

We are concerned with these insulin microspheres in a dry powder inhaler that operates under ambient conditions. As the humidity of ambient air varies markedly with location and time of year, it is important that the materials for construction have a low interaction with the particles over a wide range of humidities. This work examined the interactions between insulin microspheres and a set of five potential construction polymer materials as a function of relative humidity. The particle surface interaction forces were directly measured with a colloidal probe microscope (Butt, 1991; Ducker et al., 1991; Rabinovich et al., 2000a,b; Yang et al., 2007, 2008), which has previously been applied to similar tasks of measuring interactions between drug particles and interfaces (Eve et al., 2002; Price et al., 2002; Davies et al., 2005; Madden et al., 2006a,b). The use of AFM for measuring the interaction forces between colloidal particles and interfaces involves adhering a colloidal particle to an AFM force sensitive cantilever, as shown in Fig. 1. With a large colloidal particle as the AFM tip, the researcher will not be obtaining high-resolution images. However, one important advantage is that the particles are the actual colloidal particles of interest, and not a model surface made to emulate the particle. Furthermore, with properly designed experiments it may be possible to make measurements on several substrates or under several different environmental conditions with the same particle and on the same cantilever. This will produce data that is ideally suited for relative comparisons. One notable disadvantage of adhesion measurements with AFM in general, is the lack of knowledge concerning the tip morphology and elasticity. This is true for colloidal probe measurements as well, and using well-characterized spherical particles can alleviate some portion of this problem. While progress has been made in characterizing the colloid probe contact area with tip calibration grids, determining that the Young's modulus of the particle from a specific formulation requires more effort and is beyond the scope of this work.

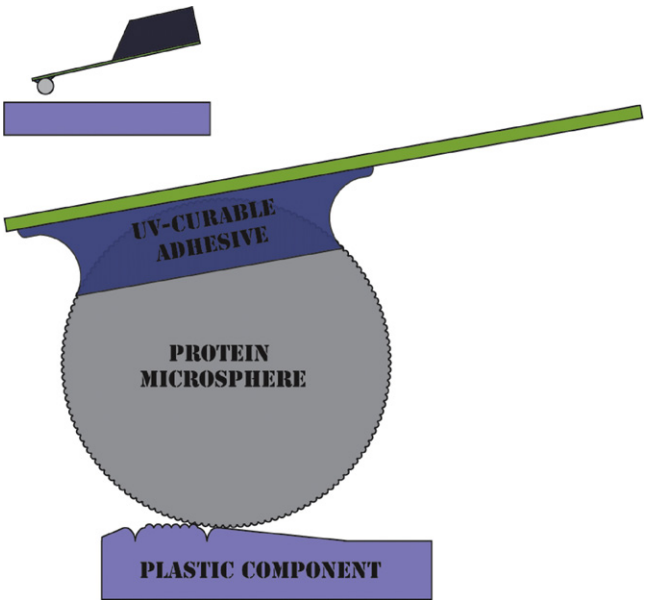

Fig. 1. This cartoon depicts colloidal probe force microscopy.

2. Materials and methods

2.1. Insulin microsphere characterization

The insulin spheres used for our experiments were provided by EPIC Therapeutics Inc. and were fabricated according to the

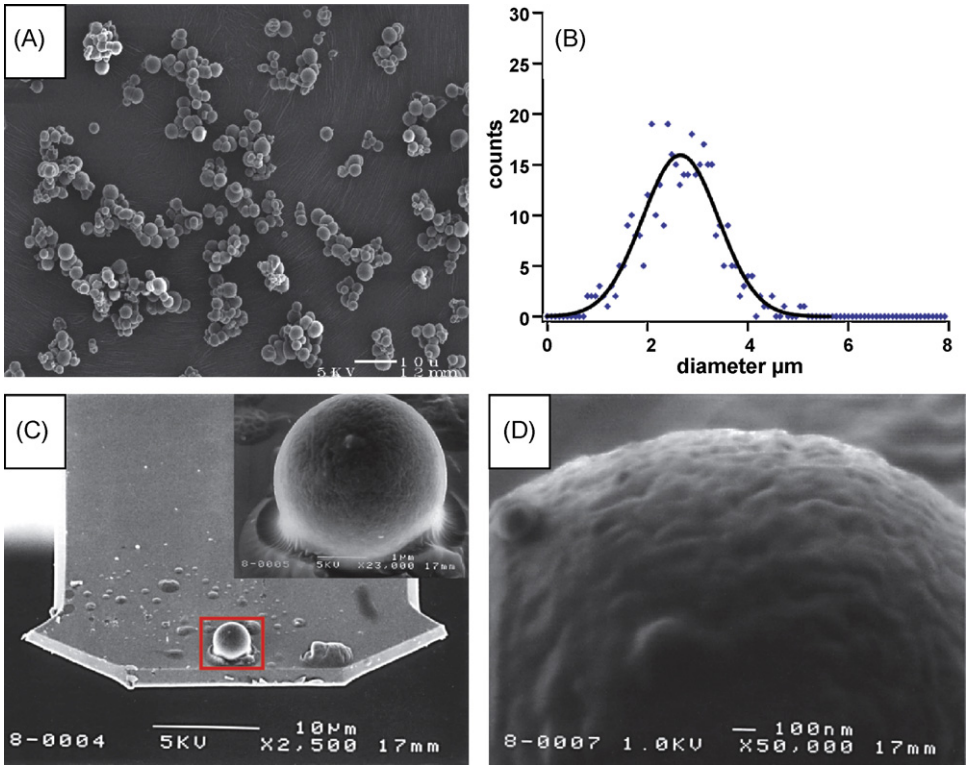

Fig. 2. SEM images insulin particles. (A) A representative distribution of microspheres, (B) a close up of a microsphere showing the surface morphology and microcrystallite arrangement, (C) a low resolution image showing the placement of the microsphere on a cantilever, (D) a higher resolution image showing the active area of the probe which was used for force measurements (both of these SEM images were performed following the force measurements.

PROMAXX process (Bromberg et al., 2005). Fig. 2A shows a scanning electron microscope (SEM) image of a representative group of this specific lot of 2–5 μm diameter insulin spheres. A histogram of particle diameters from 377 spheres is shown in Fig. 2B, and represents a population with a mean and standard deviation of 2.6 ± 1.1 μm, respectively. Examination of the particle morphology utilizing a higher resolution SEM revealed the presence of surface texture, shown in Fig. 2C and D. Both the particle size distribution and the surface roughness are expected to have an impact on delivery performance, and this will be discussed more below. All SEM images were obtained with a JSM-6300F field emission SEM operating at ≤5 kV. A Denton Desk IV vacuum sputtering system equipped with a rotating-tilting sample stage was used to deposit a thin film of palladium on the samples just prior to SEM imaging. In the case of cantilever-supported particles, this coating was, of course, preformed by following the force measurements.

2.2. Polymer characterization

The devices were designed to perform at all ambient humidity conditions, and as such the study focused on hydrophobic polymers. The five specific polymers were (1) polytetrafluoroethylene (PTFE), (2) polyethylene (PE), (3) polypropylene (PP), (4) polyethylene with an antistatic additive (PEa) and (5) polypropylene with an antistatic additive (PPa). The PTFE was obtained from McMaster-Carr (Extreme-Temperature Slippery PTFE) in the form of a 0.0625" thick sheet. The 0.5" diameter PTFE sample discs were punched out of this sheet with a circular hole punch. The other polymers were prepared on site by first injection molding of the appropriate polymer blend into large discs (2.5" diameter and 0.045" thick). The actual polymer sample discs were then created by punching out 0.5" diameter discs. The polyethylene was created from high-density polyethylene (Chevron Phillips PE HiD 9012), which was mixed with a white colorant (PolyOne CC00018445DR) at a ratio of 96:4::HDPE:colorant. The polyethylene with additive was created by blending this colored polyethylene with Dow Entira™ AS antistatic additive at a ratio of 80:20::PE:additive. The polypropylene was formed in a similar manner by blending polypropylene (Huntsman 13R9A) with a blue colorant (PolyOne CC00018615DR) at a ratio of 96:4::PP:colorant. The polypropylene with additive was formed by blending this colored polypropylene and the Dow Entira™ AS at a ratio of 80:20::PP:additive. All compositions were blended as pellets, with ratios determined by weight, and no release agents were used.

Each of the five polymer samples was rinsed with isopropanol, IPA (B & J, high purity grade) and blown dry with a stream of tetrafluoroethane (Cleantex, MicroDuster III). In an effort to make measurements as accurate and reproducible as possible, all five polymers were mounted into the AFM at the same time. Given the small sample size permitted in the Nanoscope MultiMode configuration, the polymer discs required additional processing. Each of the cylindrical sample discs was cut into six 60° wedges using a microtome blade (Crescent Mfg. Co, Duraedge), and one wedge from each material was mounted side by side on a single 12 mm diameter stainless steel AFM sample puck (SPI supplies, West Chester PA). The samples were held in place with a film of dental wax (Electron Microscopy Sciences, Nu-Base), as shown in Fig. 3A. By embedding the samples in the dental wax, the surfaces of samples with dramatically different thicknesses were presented to the AFM tip in essentially the same geometric plane. In this way, measurements on all samples could be performed under essentially identical temperature and relative humidity conditions.

Before making interaction force measurements, each of the samples was characterized by optical microscopy and with tapping mode AFM. All AFM measurements were performed with a Veeco Multimode AFM and a Nanoscope V controller. The AFM was equipped with a 120-micron scanner, which was calibrated immediately prior to use. The tapping mode cantilever (Veeco, model TESP) has the following manufacturers specifications: $f = 280–320$ kHz, $k = 20–80$ N/m, $R_{tip} < 10$ nm, $H_{tip} = 10–15$ μm.

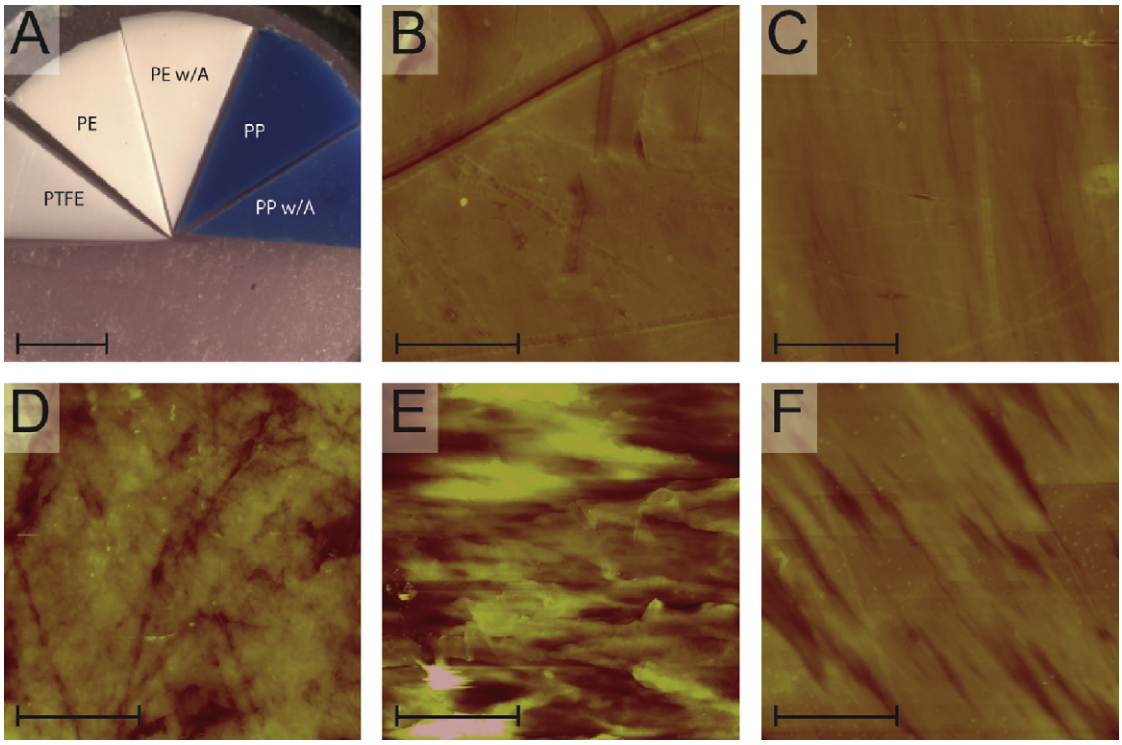

Fig. 3. Polymer substrate sample design and topographical images of all five different substrates. (A) The sample arrangement facilitating more rapid and comparable force measurement at different ambient conditions, all images are 30 μm tapping mode AFM images of (B) polyethylene, (C) polyethylene with antistatic additive, (D) polypropylene, (E) polypropylene with antistatic additive and (F) PTFE. Each of these images is centered over the region where force measurements were performed.

The cantilever was rinsed with IPA and blown dry and was used without further characterization. The cantilever can be positioned above any point within the central 2 mm of the sample puck, and a episcopically illuminated optical microscope recorded the alignment of the cantilever with features on the sample. The regions of each polymer substrate chosen for tapping mode imaging which are shown in Fig. 3B–F and defined the locations where adhesion measurements would be performed. The tapping mode images were acquired over a 30.0 μm × 30.0 μm square at a scan rate of 0.498 Hz, and feedback amplitude equal to 0.85 of the cantilever free amplitude.

2.3. Cantilever characterization and modification

A tipless AFM cantilever (Micromasch NSC12/tipless/NoAl) was used for insulin microsphere—surface interaction measurements. This cantilever had a resonant frequency of 116.8 ± 0.9 kHz, and its force constant was determined to be 2.14 ± 0.03N/m by using the added mass method (Cleveland et al., 1993), see supplementary data for a detailed description. Briefly, we modified this method by using NIST certified polystyrene microspheres, and by precisely positioning the spheres along a line at the length where the insulin microsphere was to be attached. These spheres were not attached to the cantilever and could be readily dislodged with mechanical action. Following calibration, a microscopic droplet of UV curable adhesive (Loctite, 3921) was placed on the end of the tipless cantilever using a camelhair brush mounted in a homebuilt micromanipulator and visualized with a diascopically illuminated optical microscope (Nikon, Optiphot-2). One of the larger particles was chosen and was affixed to the adhesive at the end of the tipless cantilever. This particle was fixed to the cantilever by a 30 s exposure to the 254 nm wavelength of a UV lamp (UVP, model UVGL-25). The cantilever-supported particle was used for force measurements, as described below, and then was characterized by high resolution SEM imaging as described above. Images of the cantilever supported particle are shown in Fig. 2C and D.

2.4. Humidity control of AFM head

The force measurements were made in the atmospheric tapping mode cantilever holder, with a Parafilm M® (American National Can) seal covering the front of the AFM head. The humidity of the air that was used to purge the AFM head was controlled and monitored as described below. Dry air passed through two separate rotameters (Gilmont, #1745), and after one path led air through a water bubbler the two streams were combined, at which point they flowed together through ~2 meters of tubing, past a thermal/humidity probe (Vaisala, HM-34) just before entering the AFM head. The ratio of the dry and wet streams were adjusted with needle valves to tune the measured humidity from 0 to 80% RH, while keeping the total flow rate ~700 mL/min. We typically purged the AFM head for 15 min prior to making measurements, and this corresponds to purging the head with ~100× the head volume. For a given set of force measurements the humidity did not fluctuate more than 0.1%RH from the recorded value, and the temperature for the entire set of experiments was stable at 20.6 ± 0.2 °C.

2.5. Force measurements

The cantilever-supported particle was mounted in the humidity controlled AFM, and the cantilever resonant frequency was measured, f_o = 114.53 kHz. The cantilever was visually aligned (to within a ±5 μm) above the center of the previously imaged location of the polyethylene sample, the AFM scan size was set to zero, and the cantilever was engaged at a small deflection force of ~2nN. Immediately after engagement, the AFM was set to acquire force–distance curves (force curves).

The force curves were executed with the following settings: scan rate = 1 Hz; trigger deflection value = 10 nm (21 nN); scan size = 100, 500 or 1000 nm; delay upon extend = 10 ms; a delay upon retract = 10 ms; and 8192 datapoints/force curve. The deflection sensitivity was measured at a high enough trigger force to produce a linear relationship between the cantilever deflection and the piezoelectric scanner displacement. Next the microscope was set to Force Volume® mode, and separate force curves were measured at a square grid of locations covering a 3 μm square with 32 × 32 force curves. The settings for the force volume imaging were the same as those used for the force curves. The cantilever deflection and the z-piezo voltage were also recorded with a Tektronix 5034B digital phosphor oscilloscope, which was able to stream every force curve straight to a hard drive. A homemade data analysis program, written for IgorPro (Wavemetrix), was used to extract and analyze the force data from the Force Volume® data file (see supplementary data for program listing). The program determined the difference between the approach and retract portions of the force curves, and then measured the pull-off deflection, which was directly converted into the pull-off force. The program also computed the histogram of the 1024 force curves, and fit the histogram with a Gaussian distribution.

Following acquisition of the force volume image over the polyethylene at the dry humidity of 0.5% RH, the cantilever was withdrawn and positioned above the antistatic polyethylene sample. The process was repeated and the tip was then moved on to the polypropylene, then the antistatic polypropylene and finally to the PTFE. Once the PTFE sample was examined the humidity was changed to ~20%, as described above, and the entire cycle of measurements was repeated. In this way the humidity was changed to 40, 60 and finally 80% RH.

3. Results

Representative data for insulin-polypropylene interactions are presented in Fig. 4. The force curves are combined and plotted as a two-dimensional map of adhesion forces between the insulin microsphere and polypropylene substrate. The 1024 individual adhesion force measurements are also plotted as a histogram in Fig. 4, and the histogram is fit with a Gaussian distribution. By simultaneously acquiring some low-resolution height information, correlations of adhesion with surface topography become evident. Examination of the height and pull-off force maps in Fig. 4 shows the expected strong negative correlation between the surface curvature and the pull-off force in a 3 μm square window, as features that are tall and sharp tend to have lower adhesion, while valleys tend to exhibit larger pull-off forces. This analysis was repeated for each humidity-polymer combination, and the resulting 25600 individual pull-off force measurements as a function of humidity for each polymer substrate is shown in Fig. 5. The error bars of Fig. 5 correspond to the standard deviations of the Gaussian fits to the histogram data.

A few key observations can be made from direct inspection of Fig. 5. First, the propylene with antistatic additive had a significantly lower pull-off force at the lowest RH compared to the other test polymers. Second, PTFE had the highest adhesion forces in the 20–40% RH regime compared with the other polymers that maintained very low pull-off forces over the same RH. Finally, at 80% RH, the adhesion force measurements for the different polymers appeared similar and relatively low (<50 nN). These results demonstrate that the colloidal probe microscope can be utilized to differentiate between potential construction materials for drug delivery devices, and in this case, describe insulin microsphere interactions with model dry powder inhalation device materials.

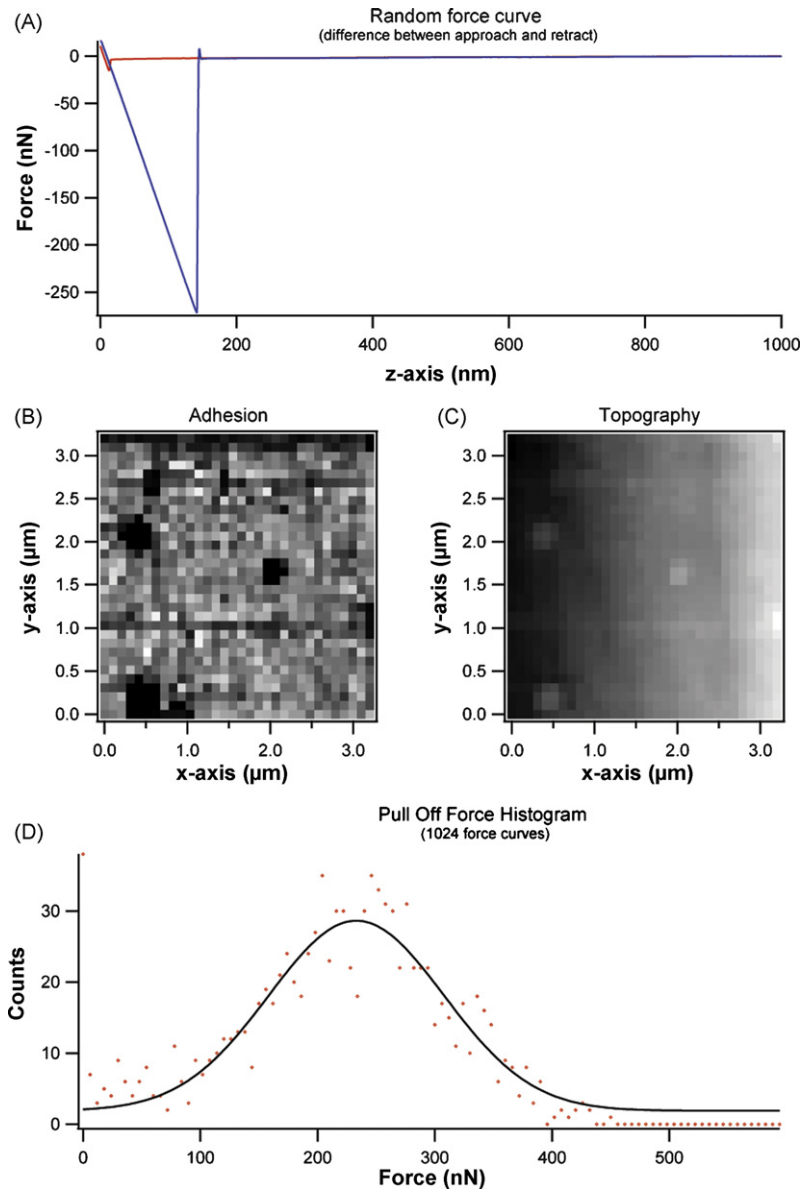

Fig. 4. Pull-off force measurements for insulin microsphere–polypropylene interactions measured at 0.5% relative humidity. (A) A representative force curve for the insulin–polypropylene interaction, (B) the pull-off force image of the same area, (C) a topographical image of the area where these force measurements were performed, (D) the histogram of 1024 pull-off forces from that area.

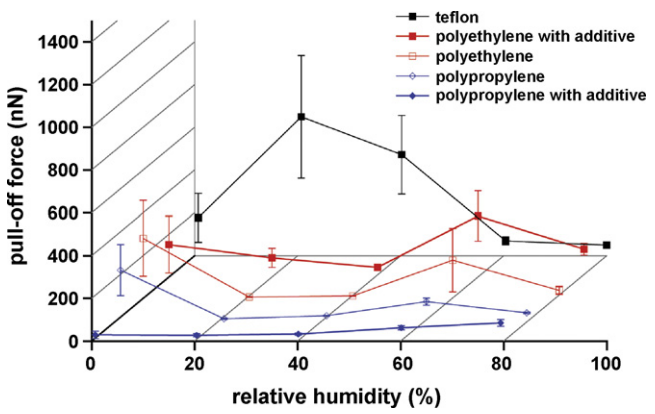

Fig. 5. Composite pull-off force as a function of humidity for all five polymer substrates. The pull-off force depends upon the humidity, and of the five different samples, only the polypropylene with the antistatic additive gave consistently lower pull-off forces over the entire humidity range.

4. Discussion

The core data of this report is centered on the comparison of the pull-off forces for five different construction materials with insulin as a function of the relative humidity, given that the inhalation based devices could be used under a wide range of ambient conditions. Polypropylene with antistatic additive performed best due to its consistently lower pull-off force over the whole humidity range sampled. This material behavior in a device would be expected to retain less of the insulin microspheres and dose most consistently across a range of relative humidities. It is hypothesized that at the highest relative humidities, water sorption at the insulin and polymer surfaces dominates to yield similar adhesion force measurements. At lower relative humidities, the surface chemistry, topography, and charging effects appear to play a more significant role. While actual device performance data to correlate with adhesion data does not exist, a number of experimental design considerations have been implemented that help enable this interpretation.

Direct comparison of force measurements is most properly performed with the same cantilever, microsphere tip, test polymer morphology, and at the same relative humidity. These factors drove the experimental plan to a parallel design, with all five substrates mounted in the AFM at the same time. In this way, we could use the same cantilever with the same microsphere and rapidly change between samples, without breaking the humidity seal. This however is a time consuming and error introducing action. Although we controlled the above factors, each sample still presented its own surface roughness, as seen in Fig. 3. All of these height images have a 1.0 μm vertical color table (from black to white) with the same contrast, and so direct comparison of the color between images is allowed. The surface roughness can be used to separate the samples into three groups (1) the roughest (polypropylene with the antistatic additive); (2) those with intermediate roughness (the polypropylene and the PTFE); and (3) the smoothest (the polyethylene with and without additive). The surface roughness of these parts does not reflect any innate property of the construction materials, but is instead more a measure of the methods used to make these specific parts. Since individual polymer surface roughness does not change, the humidity dependent adhesion behavior reflects more complex behavior than simple surface roughness effects. In an effort to further mitigate the impact that roughness and chemical heterogeneity have on the precision of force measurements, we used optical microscopy to align the microsphere-sample contact so as to limit the contact to the centers of the tapping mode images.

Additional steps were taken to help eliminate systematic errors. We performed force measurements on each sample at a given humidity value, and then we incremented the humidity, allowed it to equilibrate, and then made measurements on all of the samples again. If the tip shape or chemistry were to undergo a transformation, we would expect it to impact all of the interaction measurements similarly; however, the steady increase of the force with humidity for the polypropylene with additive sample supports the hypothesis that the tip was stable during these measurements, and that the substantial pull-off force variations observed with the other substrates are real. Thus, the combination of surface roughness and surface chemistry appear likely to impact particle–device adhesion. Surface roughness will influence not only particle–device interactions but particle–particle interactions as well.

When considering dry powder inhalation as a delivery strategy, uniform slightly rough spherical particles have several advantages. The SEM images of the insulin microspheres in Fig. 2 show that the particles tend to be spherical, and that the surface texture appears relatively smooth. When compared to most protein and pharmaceutical micronized particles, these microspheres exhibit positive qualities that will tend to improve the dispersion into air streams. The uniform convex shape leads to less mechanical locking and irreversible aggregation, and a slightly roughened texture will tend to lower adhesion with opposing surfaces, due to the reduction of contact area caused by the higher radii of curvature at the asperities. The exception to this is can occur when considering interactions between two similarly rough surfaces, if the topography of the opposing surfaces tend to mate with each other, then the interaction force is expected to markedly increase, due to the substantial increase in the contact surface area. Overall, the spherical microparticle geometry used in these studies was advantageous for maintaining consistent, reproducible contact areas with the polymer surface that can be compromised for more irregular particle geometries with repeated surface collisions.

Accurate force measurements also required that the cantilever force constant be calibrated, and while there are several common methods, we chose to use the added mass method (Cleveland et al., 1993), shown in the supplementary data. This method is generally considered to be difficult and not very reproducible; however, by making use of NIST certified polystyrene microspheres, we were able to quickly and easily generate very linear calibration curves with random residuals. The real advantage comes from avoiding the need to measure the particle diameter with an optical microscope. While the thermal method is definitely faster to implement, the inclusion of mechanical noises in with the thermal component can lead to systematic errors, while the use of NIST certified microspheres reduced the systematic and random errors. The placement of the microspheres on the cantilever is very important, and we found that arbitrary placement led to substantial scatter in the data, while precise placement enabled a substantial improvement in the reliability of the data and improved the confidence of the fit.

5. Conclusions

The dispersion of pharmaceutical particles within dry powder inhalers and the subsequent transport to the alveolar space is a complicated and multivariate problem. Optimizing delivery would require an understanding of the particles (size, shape, compliance, surface chemistry and energy), the device (roughness, compliance, surface chemistry, and energy), the environment (temperature, gas composition, and humidity), as well as the complex manner in which these variables interrelate. Nonetheless, efforts to deconstruct the problem and to understand the primary sources for the particle dynamics continue. AFM and more specifically colloidal probe microscopy can generate direct measurements of particle–surface interaction forces. The insulin microspheres had a significantly lower pull-off force at 1% RH with the antistatic polypropylene as compared to the other test polymers. The PTFE had the highest adhesion forces with insulin at 20–40% RH, and generally exhibited large long-range electrostatic attractions. At 80% RH, the adhesion force measurements for the different polymers were quite similar. The force required to remove a microsphere from a PTFE surface would be excessive over most of the humidity range, making PTFE a poor choice of building material. While both of the polyethylene materials produced low microsphere-surface forces over mid range %RH, both dry and humid extremes resulted in large forces that would limit applicability. The polypropylene surfaces both exhibited low forces at high humidities, but the polypropylene with additive produced low forces over the entire humidity range tested. Of the five potential construction materials, the polypropylene with Entira AS additive is clearly the best choice based on minimization of the insulin microsphere pull-off force over a wide range of humidities. Interpretation of the data can be effectively understood from contact mechanics and the interplay of surface chemistry and surface roughness, although practical implementation will definitely require additional experimentation.

Acknowledgment

The authors thank Dr. Kristy Wood of Baxter International for supplying the insulin microspheres.

Appendix A. Supplementary data

Supplementary data associated with this article can be found, in the online version, at doi:10.1016/j.ijpharm.2009.01.004.

References

Agu, R.U., Ugwoke, M.I., Armand, M., Kinget, R., Verbeke, N., 2001. The lung as a route for systemic delivery of therapeutic proteins and peptides. Respir. Res. 2, 198–209.

Bromberg, L., Rashba-Step, J., Scott, T., 2005. Insulin particle formation in supersaturated aqueous solutions of poly(ethylene glycol). Biophys. J. 89, 3424–3433.

Butt, H.-J., 1991. Measuring electrostatic, van der Waals, and hydration forces in electrolyte solutions with an atomic force microscope. Biophys. J. 60, 1438–1444.

Cleveland, J.P., Manne, S., Bocek, D., Hansma, P.K., 1993. A nondestructive method for determining the spring constant of cantilevers for scanning force microscopy. Rev. Sci. Inst. 64, 403–405.

Davies, M., Brindley, A., Chen, X., Marlow, M., Doughty, S.W., Shrubb, I., Roberts, C.J., 2005. Characterization of drug particle surface energetics and Young's modulus by atomic force microscopy and inverse gas chromatography. Pharm. Res. 22, 1158–1166.

Ducker, W.A., Senden, T.J., Pashley, R.M., 1991. Direct measurement of colloidal forces using an atomic force microscope. Nature 353, 239–241.

Eve, J.K., Patel, N., Luk, S.Y., Ebbens, S.J., Roberts, C.J., 2002. A study of single drug particle adhesion interactions using atomic force microscopy. Int. J. Pharm. 238, 17–27.

Hickey, A.J., Mansour, H.M., Telko, M.J., Xu, Z., Smyth, H.D.C., Mulder, T., McLean, R., Langridge, J., Papadopoulos, D., 2007. Physical characterization of component particles included in dry powder inhalers. I. Strategy review and static characteristics. J. Pharm. Sci. 96, 1282–1301.

Madden, C.E., Collins, J.A., Roberts, C.J., Swaminathan, V., Joshi, V., Gray, S., 2006a. Measurement of particle deformation and electrostatic force using atomic force microscopy (AFM). Respir. Drug Deliv., 695–698.

Madden, C.E., Collins, V., Joshi, J.A., Roberts, C.J., Gray, S., Bennett, D., Swaminathan, V., 2006b. Measuring particle interactions in a dry powder insulin inhalation product using atomic force microscopy (AFM). Respir. Drug Deliv., 699–702.

Mandal, T.K., 2005. Inhaled insulin for diabetes mellitus. Am. J. Health-System Pharmacy 62, 1359–1364.

Price, R., Young, P.M., Edge, S., Staniforth, J.N., 2002. The influence of relative humidity on particulate interactions in carrier-based dry powder inhaler formulations. Int. J. Pharmaceutics 246, 47–59.

Rabinovich, Y.I., Adler, J.J., Ata, A., Singh, R.K., Moudgil, B.M., 2000a. Adhesion between nanoscale rough surfaces: I. Role of asperity geometry. J. Colloid Interface Sci. 232, 10–16.

Rabinovich, Y.I., Adler, J.J., Ata, A., Singh, R.K., Moudgil, B.M., 2000b. Adhesion between nanoscale rough surfaces: II. Measurement and comparison with theory. J. Colloid Interface Sci. 232, 17–24.

Yang, S., Zhang, H., Hsu, S.M., 2007. Correction of random surface roughness on colloidal probes in measuring adhesion. Langmuir 23, 1195–1202.

Yang, S., Zhang, H., Nosonovsky, M., Chung, K.-H., 2008. Effects of contact geometry on pull-off force measurements with a colloidal probe. Langmuir 24, 743–748.